Korean J. Chem. Eng., 32(6), 1094-1100 (2015)
DOI: 10.1007/s11814-014-0333-7

pISSN: 0256-1115
eISSN: 1975-7220

Combination of maghemite and titanium oxide nanoparticles in polyvinyl alcohol-alginate encapsulated beads for cadmium ions removal

Zohreh Majidnia and Ani Idris†

Department of Bioprocess Engineering, Faculty of Chemical Engineering, C/O Institute of Bioproduct Development (IBD), Universiti Teknologi Malaysia, 81310 UTM Johor Bahru, Johor, Malaysia
(*Received 20 April 2014 • accepted 13 November 2014*)

Abstract−Both maghemite (γ-Fe_2O_3) and titanium oxide (TiO_2) nanoparticles were mixed at various ratios and embedded in polyvinyl alcohol (PVA)-alginate beads. These beads were tested for photocatalytic behavior in eliminating toxic Cd(II) from the aqueous solution. The photocatalytic experiments were performed under sunlight irradiation at various pH, initial feed concentrations and γ-Fe_2O_3: TiO_2 ratios. The recycling attribute of these beads was also investigated. The results revealed that 100% of the Cd(II) was eliminated in 150 minutes at pH 7 under sunlight. It shows that maghemite and titania PVA-alginate beads can be readily isolated from the aqueous solution after the photocatalyst process and reused for at least six times without losing their initial properties.

Keywords: Titanium Oxide Nanoparticles, Magnetic Nanoparticles, Encapsulation, Waste Water, Desorption

INTRODUCTION

The presence of heavy metal ions in the environment is of major concern due to their toxicity to many life forms [1,2]. Heavy metal, such as cadmium has several industrial applications and is a pollutant widely found in industrial wastewaters. Its toxicity affects the ecosystem and presents a human health risk [2-4]. The increasingly stringent European legislation on the purity of drinking water and on the concentration of contaminants present in wastewaters has created a growing interest in the development of treatment processes for the removal of hazardous metals from the aqueous solutions [1].

Titania (TiO_2) is attractive as a semiconductor because of the large surface area and pores which are considered as important in photo catalysis, chemical sensors, luminescence, self-cleaning surfaces, carbon nano tubes and solar cells [5-7]. TiO_2 is a widely used photo catalyst due to its high photocatalytic and thermostable efficiency. In recent years most of the research has focused on utilization of the TiO_2 powder for photodegrading of various organic pollutants present in polluted water and the ways of improving the catalytic properties of TiO_2 [8]. Many studies have reported on the widespread applied property of combined semiconductor materials, like that of ZnO/CdS [9] TiO_2/CdS [10] and SnO_2/ Fe_2O_3 [11].

Iron oxide nanomaterials have received much attention for their extremely small size, high surface-area-to-volume ratio, surface modifiability, excellent magnetic properties and great biocompatibility [12]. Fe_2O_3 with its band-gap of 2.2 eV is an interesting n-type semiconducting material and a suitable candidate to be used as a photocatalyst in visible light. The photocatalytic nature of Fe_2O_3 has been investigated in water splitting [13] semiconductor electrode applications and photodegradation of organic pollutants [14].

In addition, due to the narrow band-gap of Fe_2O_3, it can be used as a sensitizer of TiO_2 photocatalyst. In the presence of visible light Fe_2O_3-TiO_2 gets irradiated and the electrons in the valence band of Fe_2O_3 are excited to the conduction band and leave holes in the valence band. Due to the formation of built-in field in Fe_2O_3-TiO_2 heterojunction, the electrons present in the valence bands of TiO_2 are driven onto the Fe_2O_3 (whereas the photogenerated holes move into the valence band of TiO_2 in the opposite direction). The charge transport between the valance bands of Fe_2O_3 and TiO_2 is considered to be an effective process in promoting the photocatalytic activity of the composition, because it results in the increase of electron-hole recombination time [15].

Kuang [16] utilized Fe_2O_3 to change TiO_2 nanotube (NT) arrays with high sensitivity in the light where it is initially equipped by annealing anodic titania NTs pre-loaded with $Fe(OH)_3$ that was consistently attached to the titania NTs by utilizing sequential chemical bath deposition (S-CBD). The photo electrochemical performance of the composite nanotubes was identified by calculating the present and photogenerated voltages in the light of UV-vis. Fe_2O_3 change the titania NTs to reveal a higher photo potential and photocurrent charges than those of unchanged titania NTs. Liu [17] studied Fe_2O_3-TiO_2 composite and revealed the influence of iron oxide (Fe_2O_3) on titanium dioxide (TiO_2) in synthesizing visible light to sensitive photocatalysts. The improved sample of photocatalytic activity was greater than that of pure TiO_2 when eliminating uranium in solar light and visible light irradiation. This sample led to a photodegradation efficiency of about 90% and 40% of the uranium under visible light and solar light, respectively. Zhao et al. [18] conducted a study on TiO_2/Fe_2O_3 core-shell nano composition film that was fabricated using a two-phase method. The photoelectrochemical (PEC) implementations of the prepared composite nanorods (NR) were verified by calculating the photogenerated flows in the lighting of UV-vis light. The TiO_2 NRs which

†To whom correspondence should be addressed.
E-mail: ani@cheme.utm.my

were modified by Fe_2O_3 revealed a photocurrent charge, which was greater than that of unmodified TiO_2 NRs.

Jeong et al. [19] used adsorption properties of Fe_2O_3 and found it can be good and inexpensive adsorbents for As(V) removal in drinking water despite their relatively small surface area. In another study [21], the maximum As(V) uptake values at pH 6 - the optimal pH value for adsorption using Fe_2O_3 was calculated as 0.66 mg/g. Another composite adsorbent, which consists of iron oxide coated zeolite (IOCZ), was characterized and employed for the removal of Cu(II) from aqueous solution using fixed bed column; their findings revealed that IOCZ was an effective adsorbent for removal of Cu(II) from aqueous solution. In another research [20], multiwall carbon nanotube (MWCNT)/iron oxide magnetic composites were prepared for adsorption Ni(II) and Sr(II), and these metal ions can adsorb up to 90% of the metals. In some cases only activated carbon fiber was used in heavy metal removal such as Cr(VI) [21].

Recently, the use of photocatalyst such as γ-Fe_2O_3 nanoparticles in polyvinyl alcohol (PVA) alginate beads has been used for the reduction of metals such as Cr(VI) and Cd(II) [22,23]. They have also been used for removal of Pb(II) and other heavy metals as adsorbents [24]. Also, TiO_2 nanoparticles alone in PVA-alginate beads have been used for the removal of Cd(II) [25]. Therefore, in the current work, a combination of γ-Fe_2O_3 nanoparticles and TiO_2 nanoparticles are embedded in PVA-alginate as matrix and used as photocatalyst for the removal of Cd(II). However, to the best of our knowledge, a combination of both photocatalyst TiO_2 and γ-Fe_2O_3 has not been used extensively either as adsorbents or photocatalyst for the removal of cadmium. It is hoped that such a combination will enhance the photocatalyst beads performance and reusability.

MATERIALS AND METHODS

1. Materials

All the chemicals such as iron (II) chloride, iron (III) chloride, acetone, hydrochloric acid, ammonia solution, nitric acid, tri-sodium citrate, polyvinyl alcohol (PVA), sodium alginate, calcium chloride, boric acid, titanium isopropoxide, acetyl acetone, urea were purchased from Sigma-Aldrich and Cd(II) solution and ethanol were purchased from Merck.

2. Methods

2-1. Preparation of TiO_2 Nanoparticles

Initially, 2 ml of titanium isopropoxide and 2 ml of acetyl acetone were added to 40 ml ethanol solution and stirred continuously at room temperature. In another beaker containing 10 ml of deionized water, 0.5 g of soluble urea was added and dissolved properly. Both of these solutions were then added in drops to 40 ml of deionized (DI) water with continuous stirring until a pale yellow solution was formed with pH 5.6. The solution was continuously agitated for at least one hour and then transferred into the 120 ml Teflon coated stainless steel autoclave and heated at 150 °C for 18 hours. The content was cooled to room temperature and the yellowish white colored sample obtained was washed with ethanol and deionized water, and then finally centrifuged. The sample was dried at 80 °C for 3 h and stored in a dark colored bottle until further use [26].

2-2. Preparation of γ-Fe_2O_3 Nanoparticles

The maghemite (γ-Fe_2O_3) nanoparticles were produced through co-precipitation of stoichiometric combination of ferric and ferrous chlorides in ammonium hydroxide solution and the initially acquired magnetite (Fe_3O_4) precipitate was acidified using nitric acid and then oxidized into maghemite (γ-Fe_2O_3) at 90 °C in the presence of iron (III) nitrate. Additionally, the particles were coated with citrate anions to achieve unchanging maghemite distribution, which is well matched with alginate gel as neutral medium. Subsequently, the coated nanoparticles were distributed in water after precipitation with acetone to maintain a constant pH 7 for the ferro fluid The maghemite nanoparticles characteristics were defined in accordance with previous work [27], and the obtained maghemite was coated using citric acid and dispersed in water as similar to that of citrate ferro fluids.

2-3. Preparation Maghemite and Titania PVA-alginate Beads

Maghemite nanoparticles were mixed with titanium oxide nanoparticles at different proportion, and 100 mL of precursor solution was prepared using 12 g of PVA, 0.1 g of titanium oxide nanoparticle and 1 g of alginate in the presence of deionized water. After this 12 g of PVA was dissolved using 72 mL of distilled water and heated at 80 °C for 5 hours. PVA was also heated in microwave for 4 min to confirm entire dissolution. Meanwhile, alginate was dissolved in 20 mL of deionized water in another beaker. The PVA and alginate solution were then mixed together. The maghemite and titanium nanoparticles were then added to the PVA alginate solution to ensure that the nanoparticles were homogeneously distributed. The solution was then pumped via a peristaltic pump and dripped into a solution containing 2% of calcium chloride ($CaCl_2$) and 6% of boric acid. The obtained beads were kept in the solution for 24 hours, washed several times with distilled water and finally kept in deionized water until further use [22].

2-4. Characterization of Nanoparticles and Beads

Phase identification of the TiO_2 nanoparticles was by X-ray diffractometer (XRD, Bruker D-8 Advance) using Cu K_α radiation at wavelength, α=1.5406 °A. The morphological and structural analysis of the samples involved using field emission scanning electron microscopy (FESEM, Hitachi S4800) and also high resolution transmission electron microscopy (HRTEM, JEOL-JSM-6360). Fourier transform infrared spectroscopy (FTIR) was used to obtain the FTIR spectrum (600-3,500 cm^{-1}) for the titanium oxide nanoparticles (TiO_2).

The metal ion concentration present in the solution was determined in accordance with air-acetylene method with atomic absorption spectrophotometer (AAS). Morphological and structural analysis of the samples was by using field emission scanning electron microscopy (FESEM, Hitachi S4800) and high resolution transmission electron microscopy (HRTEM, JEOL-JSM-6360), respectively. In addition, a complementary test was performed on the alginate bead to determine the Brunauer-Emmett-Teller (BET) surface area, pore diameter and volume of alginate beads using N_2 adsorption isotherms at 80 °C with Quantachrome NovaWin 2 analyzer. X-ray photoelectron spectroscopy (XPS) was used (spectrometer (ESCALAB-2, Great Britain) equipped with an Mg Ka X-ray source (1253.6 eV)) to characterize the cadmium ions treatment.

2-5. Photocatalytic Activity under Sunlight

The experiments were performed under sunlight irradiation. 10 g of maghemite and titania PVA-alginate beads were employed

in 200 ml of Cd(II) solution in a 500 ml flask. For every 20 minutes, 5 ml of sample was analyzed for Cd(II). The initial concentration of Cd(II) present in the solution was in the range of 50, 100 and 200 mg/*l*, and the influence of pH on Cd(II) sorption was determined at different pH range of 2.5 to 10.0. The preliminary solution pH can be changed by the addition of HCl for acidic solution or NaOH for alkaline solution [28].

2-6. Desorption Experiments

The reusability of maghemite and titania PVA-alginate beads was evaluated using adsorption-desorption cycles. The experiments were repeated by using the same maghemite and titania PVA-alginate beads. The metal-loaded maghemite and titania PVA-alginate beads (10 g) were agitated in an orbital shaker for 60 min at room temperature in the presence of desorbing agent (HCl 50 ml, 0.1 M) contained in a 250 ml Erlenmeyer flasks. The obtained supernatant was analyzed for metal ion desorption using AAS. The maghemite and titania PVA-alginate beads were once again recycled and used as regenerated sorbent for five repeated sorption-desorption cycles to investigate the regenerate behavior of the adsorbent [24].

RESULTS AND DISCUSSION

1. Morphology of Nanoparticles

The maghemite nanoparticles used in this experiment have similar properties as compared to our previous work reported [27]. The XRD pattern of the TiO_2 powder obtained from the hydrothermal treatment is shown in Fig. 1. The peaks were found from (1 0 1), (0 0 4), (2 0 0), (1 0 5), (2 1 3), (1 1 6), (2 1 5), (3 0 3) reflections and the obtained reflection peaks can be indexed to anatase TiO_2 with lattice constants of a=3.784 °A and c=9.512 °A (JCPDS: no. 84-1286). Also, no characteristic peak was relevant to other crystalline forms as identified from the XRD pattern.

The FTIR spectra obtained for TiO_2 powder are shown in Fig. 2. The broad band (3,200-3,600 cm^{-1}) observed from the sample relates to the O-H stretching and deformation vibrations of weak-bound water. The bands appearing between 400-800 cm^{-1} are mostly related to the vibrations obtained from tin oxide [29], whereas the sharp bands appearing in the range of 1,400-1,700 cm^{-1} are mostly attributed to the presence of CH_2- and -CH_3 bands.

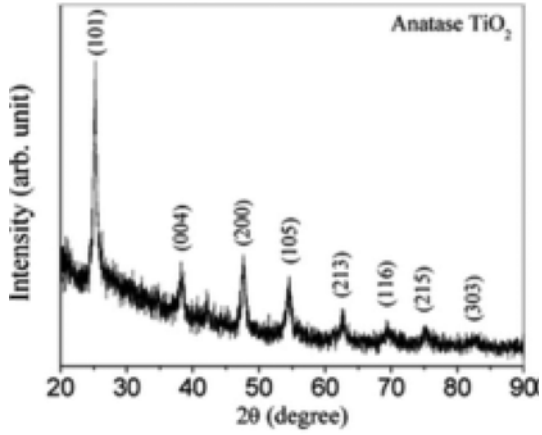

Fig. 1. XRD patterns of the prepared TiO_2 nanoparticles.

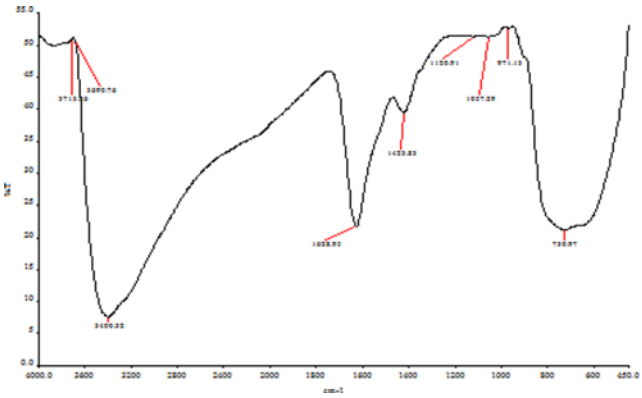

Fig. 2. FTIR analysis of TiO_2 nanoparticles.

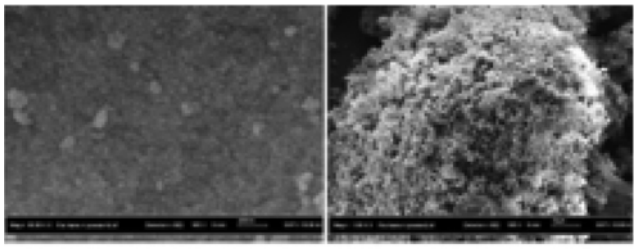

Fig. 3. FESEM images of TiO_2 nanoparticles at (a) 50 KX (b) 1 KX magnification.

The high and low magnification FESEM images of the prepared TiO_2 powder sample are in Figs. 3(a), (b). The nanoparticles are uniformly distributed throughout the sample and the particles are fairly small. Typical low and high magnification HRTEM images

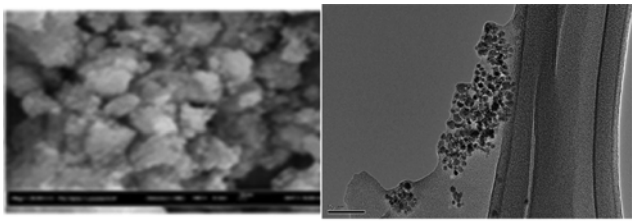

Fig. 4. TEM images of (a) TiO_2 nanoparticles (b) maghemite nanoparticles.

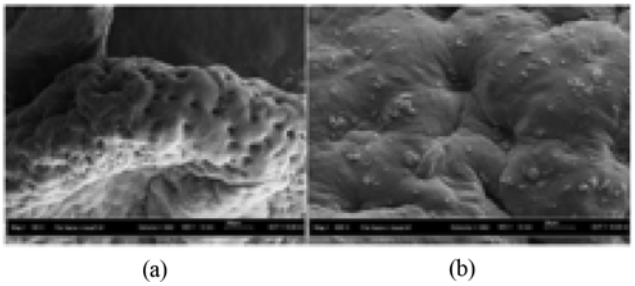

Fig. 5. FESEM surface images of maghemite and titania PVA-alginate beads (a) 100X (b) 500X.

Table 1. EDX analysis of the various elements on the surface of maghemite and titania PVA-alginate beads

Element	C	O	Ti	Fe	Ca	Na
Weight (%)	23.68	29.14	4.08	36.58	4.14	0.39

of the sample are shown in Fig. 4(a), (b), which also reveals the formation of uniform TiO_2 and Fe_2O_3 nanoparticles. The average particle sizes were 15 and 9 nm for TiO_2 and Fe_2O_3 nanoparticles, respectively (Fig. 4(a), (b)).

Fig. 5(a), (b) illustrate the surface morphology of maghemite and titania PVA-alginate beads at 100X magnification. The surface of maghemite and titania PVA-alginate beads was observed to be as porous and rough. Moreover, the EDX analysis was done in conjunction with FESEM analysis to determine the elemental composition of selected spots present in the maghemite and titania beads surface.

The EDX analysis of various elements present in the surface of maghemite and titania PVA-alginate beads is shown in Table 1. Besides Fe, Ti, Ca, and O large amounts of residual carbon were present in the initial organic component. BET surface area, pore diameter and pore volume of the maghemite and titania PVA-alginate beads were found to be 9.38 m^2/g, 1.4 nm and 7.42×10^{-2} cm^3/g, respectively.

2. Photocatalytic Activity Determination

In Fig. 6, due to the absence of maghemite and titania PVA-alginate beads, no appreciable photo-reduction occurred during the 120 minutes of irradiation, mainly because Cd(II) is stable and cannot be readily decomposed. When maghemite and titania PVA-alginate beads were added to the aqueous solution, but in the absence of sunlight, 80% of Cd(II) was removed due to the adsorption of Cd(II) onto the maghemite and titania PVA-alginate beads. However, when maghemite and titania PVA-alginate beads were added in the presence of sunlight, the reduction of Cd(II) was almost 100%, which clearly illustrates that illumination energy is essential and significant in the degradation of cadmium ions.

3. Effect of pH and Ratio on the Removal of Cd(II) Ions

The ability of maghemite and titania PVA-alginate beads to adsorb Cd(II) changes according to different pH. The pH can also determine the selectivity of compound in maghemite and titania PVA-alginate beads to proton with Cd(II) ions when compared to other ions. The influence of pH on Cd(II) binding with maghemite and titania PVA-alginate beads at different ratios of TiO_2 and Fe_2O_3 is shown in Fig. 7.

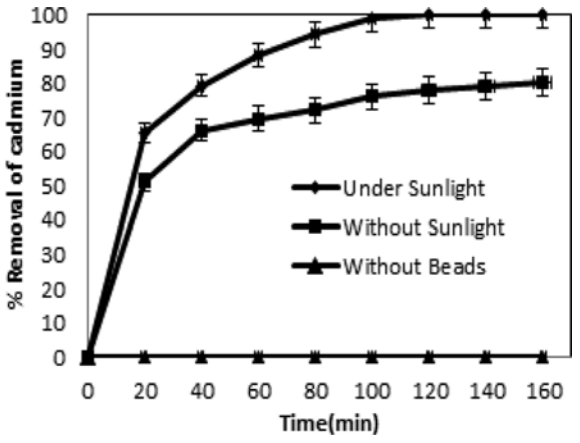

Fig. 6. Removal of Cd(II) on 50 mg/L concentration of Cd(II) at pH 7 (TiO_2 : Fe_2O_3=1).

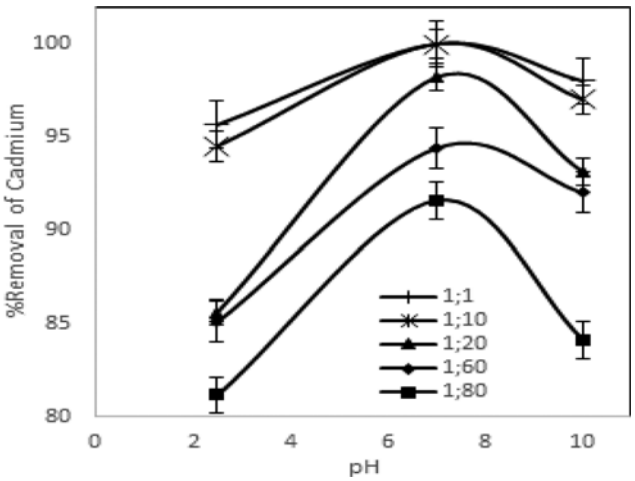

Fig. 7. Removal of Cd(II) ions by maghemite and titania PVA-alginate beads at different ratio.

The removal rate of Cd(II) steadily increased until pH 7 with increasing pH, which can be explained by the fact that at lower pH, more protons (H^+) are available to the carboxyl groups, which in turn reduces the available binding sites for alginate molecule. At pH 7, the amount of removal was observed based on maximum Cd(II) intake and a striking decrease was observed in the uptake capacity at pH 10. This is due to the formation of unstable polysaccharides and insoluble Cd(II) hydroxide, which makes the adsorption of Cd(II) ions difficult through ion exchange mechanism.

The results show that at pH 2.5, the metal sorption was low due to the competition between Cd(II) ions and hydrogen ions H^+ for protonated active sites. A similar observation was also made by Saeed et al. [30] where the heavy metal cations competed with high level of hydrogen ions available in the acidic medium to occupy negative binding sites, and was not a favorable condition for metal binding [31]. The metal ion uptake consequently increased along with increasing pH, which created negatively charged sites available for metal ion binding. Whereas, in the alkaline media the number of OH^- dominated in the solution, resulting in less competition with Cd(II) cations to bind on to the active sites. However, experiments using pH>12 were not attempted, mainly because Cd(II) ions would precipitate to form calcium hydroxides [32]. According to some papers, besides the competition binding of Cd(II) and hydrogen ions, the adsorption of metal ions also occurred through ion exchange mechanism with the replacement of calcium for the chelating of functional groups obtained from the maghemite and titania PVA-alginate beads, and one calcium ion was replaced by one Cd(II) ion during the ionic exchange process [31]. Moreover, several researchers have reported that the affinity of alginate to Cd(II) is much higher than that of Ca(II), thereby resulting in the occurrence of ion-exchange process [33]. The uptake of Cd(II) ion in the acidic medium was found to be 94.51% at pH 2.5 (TiO_2/Fe_2O_3 : 1/10), while for the alkaline test solution (pH 10), 97% of Cd(II)

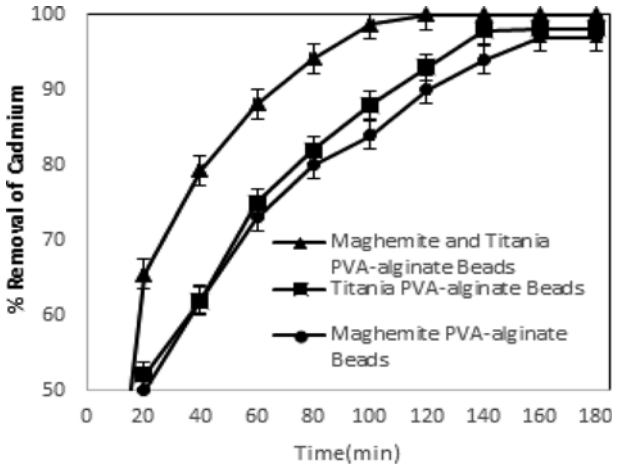

Fig. 8. Removal rate of Cd(II) for 3 different types of beads performed at pH 7 (initial Cd(II) concentration 50 mg/L, TiO_2 : Fe_2O_3=1).

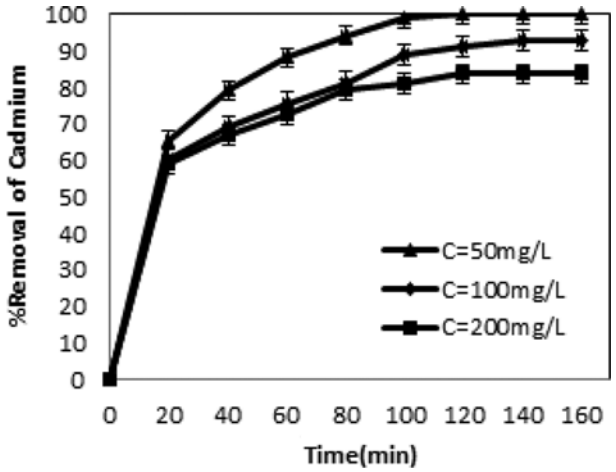

Fig. 9. Removal of Cd(II) ions with maghemite and titania PVA-alginate beads (TiO_2 : Fe_2O_3=1) at difference initial concentrations of Cd(II) in pH=7.

was found to be adsorbed, after the maghemite and titania PVA-alginate beads were introduced into the test medium. In the current study, we found that maghemite and titania PVA-alginate beads could adsorb Cd(II) ion in the pH range of 6 to 9 (Fig. 7). The maximum uptake was at neutral pH 7, with removal capacity of 100% (TiO_2/Fe_2O_3 : 1/10). The obtained results were found to be similar, where it was shown that the maximum removal of cations Cu (II) and Ni (II) onto the alginate encapsulated magnetic material beads occurred at pH 7 [31].

The removal of Cd(II) ions is very much influenced by the variation in the ratio of TiO_2 : Fe_2O_3. Fig. 8 shows the removal of Cd(II) was lowest when only Fe_2O_3 was embedded in the bead. The removal of beads was improved only slightly when only TiO_2 was embedded in the beads. However when both TiO_2 and Fe_2O_3 nanoparticles were combined in the ratio of TiO_2 : Fe_2O_3=1 and embedded in the beads the removal of Cd(II) improved significantly (100% removal within 120 minutes). Changing the ratio of TiO_2 : Fe_2O_3 to 1 : 20 did not further improve the Cd(II) removal. The excessive amount of Fe_2O_3 nanoparticles, which is in the range of 9 nm, probably blocks the pores of the maghemite and titania PVA alginate beads; thus Cd(II) ions cannot penetrate and be adsorbed by the beads. The presence of large amounts of Fe_2O_3 tend to also hinder light from reaching the photocatalyst, thereby decreasing the removal efficiency. The findings are in line with work by other researchers [28,34] who reported that excessive catalyst tends to prevent illumination of catalyst and no longer improves the performance.

4. Effect of Initial Concentration of Solution on Removal of Cd(II) Ions

The result of (Fig. 9) shows that as the metal concentration of Cd(II) ions increased, the rate of Cd(II) removal decreased. The uptake of Cd(II) ions with respect to contact time mainly occurred in two stages. A rapid metal uptake was observed during the first hour of sorbent-sorbet contact, known as the first stage, and then followed by a slower metal uptake rate occurring over a considerably longer period of time until a stable equilibrium was achieved, known as the second stage. Such adsorption pattern has been

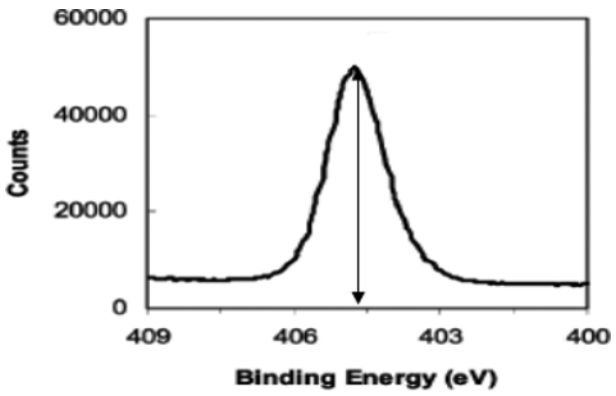

Fig. 10. X-ray photoelectron spectra for cadmium binding energy region.

reported in several literature reviews involving various other metal ions or adsorbents [32,35].

5. Mechanism of Cadmium Ions Removal

The chemical state of cadmium ions after the treatment under sunlight was characterized by XPS consecutively in high resolutions scan at 400-409 eV. The principal Cd ions XPS binding energy region was shown in Fig. 10, where the formation of cadmium zero-valent at 404.9 eV is observed. The results proved that Cd(II) was reduced to Cd(0) under sunlight and could be classified as a photocatalytic process.

Studies have shown that Fe_2O_3 has a low band gap (2.2 eV), and under sunlight irradiation γ-Fe_2O_3 nanoparticles are excited to produce electron-hole pairs [36]. When combined with TiO_2 nanoparticles, which could absorb photons with different level of energy and excite photoelectrons from the valence band (VB) to the conduction band (CB) [36], electron injection was expected from the conduction band of TiO_2 into γ-Fe_2O_3 nanoparticles since the conduction band of Fe_2O_3 is more positive than TiO_2 [37]. Therefore, the photogenerated electrons could be shuttled along Fe_2O_3/TiO_2 hetero-nanoparticles to the external circuit drove by the bias voltage, allowing charge separation and recombination suppression [26].

Also, the combination of crosslinking and entrapment of the PVA-alginate probably allows easy penetration and absorption of the photon, thus generating electron-hole pairs not only on the surface of adsorbents but also inside the matrices [22] as shown in Eqs. (1) to (3).

$$\gamma\text{-}Fe_2O_3+h\upsilon\rightarrow\gamma\text{-}Fe_2O_3\ (e+h) \quad (1)$$

$$TiO_2+h\upsilon\rightarrow TiO_2\ (e+h) \quad (2)$$

$$\gamma\text{-}Fe_2O_3+TiO_2(e)\rightarrow\gamma\text{-}Fe_2O_3(e)+TiO_2 \quad (3)$$

Thus the combined γ-Fe_2O_3 and TiO_2 produces electron hole pairs responsible for the reduction of Cd(II) to Cd(0) via the two electron reaction of Cd expressed by Eq. (4).

$$Cd(II)^{e^-}\rightarrow Cd(I)^{e^-}\rightarrow Cd(0) \quad (4)$$

6. Kinetic Studies

6-1. Pseudo-second-order Rate Model

A pseudo-second-order rate model was used to describe the kinetics of absorption of Cd(II) ions onto the adsorbent material [38], whereas the differential equation for chemisorptions kinetic rate reaction is expressed as follows:

$$q=(C_o-C_t)\frac{V}{m} \quad (5)$$

$$\frac{dq_t}{dt}=k(q_e-q_t)^2 \quad (6)$$

where k is the rate constant of pseudo-second-order equation (L/mg h).

For the boundary conditions t=0 to t=t and q_t=0 to q_t=q_t, the integrated form of Eq. (6) becomes:

$$\frac{1}{q_e-q_t}=\frac{1}{q_e}+kt \quad (7)$$

Eq. (7) can be rearranged to obtain a linear form of equation as:

$$\frac{t}{q_t}=\frac{1}{kq_e^2}+\left(\frac{1}{q_e}\right)t \quad (8)$$

If the initial sorption rate h (mg/L h) is:

$$h=kq_e^2 \quad (9)$$

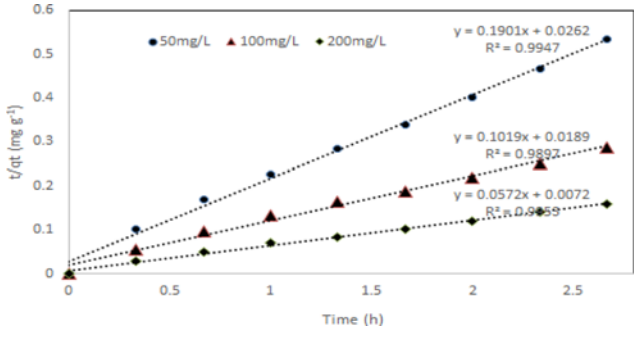

Fig. 11. Pseudo-second-order sorption kinetics of Cd(II) on maghemite and titania PVA-alginate beads at various initial concentration.

Table 2. The calculated parameters of the pseudo-second-order kinetic models for Cd(II) ions sorbed onto maghemite and titania PVA-alginate beads [Experimental condition: pH=7]

Initial conc.	q_e (mg/g)	C_{eq} (mg/L)	h (mg/g h)	k (g/mg h)	R^2
50 mg/L	5.26	0.001	38.16	1.37	0.9974
100 mg/L	9.81	7.12	52.91	0.55	0.9892
200 mg/L	17.48	32.78	138.88	0.40	0.9846

Then Eqs. (8), (9) will become:

$$\frac{t}{q_t}=\frac{1}{h}+\frac{1}{q_e}t \quad (10)$$

Fig. 11 illustrates the kinetic plots of t/q_t with respect to time for Cd(II) ion sorption at different initial concentrations. A linear relationship exists between t/q_t and t, and the correlation coefficient (R^2) was found to be greater than 0.994, which indicated a strong relationship between these parameters that the process of Cd ion sorption obeyed the pseudo-second-order kinetic model. Table 2 shows that the values of initial sorption rate 'h' and rate constant 'k_1' increase with increase in initial concentration. The extremely high R^2 (>0.99) and the theoretical q_e values were found to be in close agreement with the experimental values. Thus the prevalent mechanism is the pseudo-second-order sorption and the overall rate constant of each sorbent seemed to be governed by the chemisorption process.

7. Desorption and Regeneration Potential of Beads

The cost associated with the adsorption system is of crucial importance and is determined by the desorption and regeneration potential of maghemite and titania PVA-alginate beads. From the current study, the Cd(II) desorption from the metal-loaded maghemite and titania PVA-alginate beads occurred at pH 7 with the initial concentration of 50 mg/*l*. Findings also showed that Cd(II) desorption from the metal-loaded maghemite and titania PVA-alginate beads for the first cycle resulted in 98.01% of metal recovery. Froom Fig. 12, desorption percentage for the metals did not decrease remarkably during the six sorption–desorption cycles. The

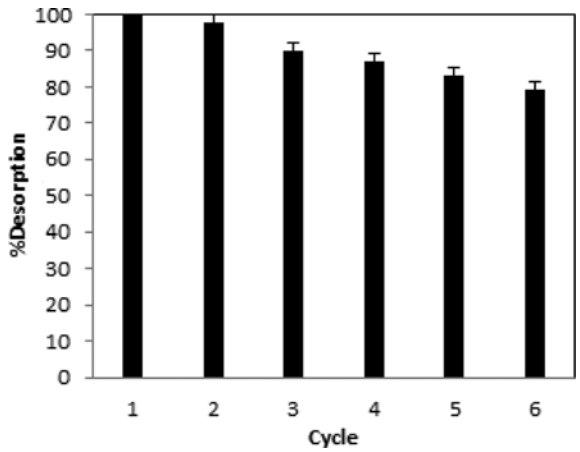

Fig. 12. Desorption capacities on recycled maghemite and titania PVA-alginate beads.

metal removal efficiency of Cd(II) on maghemite and titania PVA-alginate beads was found to be 98.01% during the first cycle, while in the second cycle showed decrease in 8.03%. After the second cycle a small decrease in the sorption capacity of maghemite and titania PVA-alginate beads was observed; however, the decrease was not too drastic. Therefore, the findings clearly indicate that maghemite and titania PVA-alginate beads can be recycled for at least six times without losing too much photocatalytic property.

CONCLUSION

The preparation of maghemite and titania PVA- alginate photocatalytic beads through immobilization of titanium oxide and magnetic nanoparticles using alginate and PVA was successfully demonstrated. It was found that the photocatalyst beads can remove 100% of Cd(II) and can be reused and recycled at least six times throughout the process. The photocatalytic properties were systemically studied. It was seen that under sunlight irradiation, Cd(II), which is being considered as a major toxic waste water pollutant, can be entirely reduced within 120 min. The results show that equilibrium can be achieved in less than 2 h within the suitable pH range of 6 to 10, where the maximum removal occurred at pH 7. The pseudo-second-order rate model was used for the mathematical description of the removal of Cd(II) ions onto maghemite and titania PVA-alginate beads. The experimental data can be fitted well with the pseudo-second-order rate model kinetic model with the R^2>0.99 to further explain the photoreduction process.

REFERENCES

1. M.Vaclavikov, P. Misaelides, G. Gallios, S. Jakabsky and S. Hredzak, *Stud. Surf. Sci. Catal.*, **155**, 517 (2005).
2. W.-W. Tang, G.-M. Zeng, J.-L. Gong, J. Liang, P. Xu, C. Zhang and B.-B. Huang, *Sci. Total Environ.*, **468-469**, 1014 (2014).
3. A. Agrawal and K. K. Sahu, *J. Hazard. Mater.*, **137**, 915 (2006).
4. H. R. Mortaheb, H. Khormaei, M. H. Amini and B. Moktarani, *Can. J. Chem. Eng.*, **91**, 1575 (2013).
5. A. Brioude, P. Vincent, C. Journet, J. C. Plenet and S. T. Purcell, *Appl. Surf. Sci.*, **221**, 4 (2004).
6. G. Ruppert, K. Hofstadler, R. Bauer and G. Heisler, *J. Chem. Sci.*, **105**, 393 (1993).
7. S. C. Jung and N. lmaishi, *Korean J. Chem. Eng.*, **18**, 867 (2001).
8. G. Colón, M. C. Hidalgo, M. Macías, J. A. Navío and J. M. Doña, *Appl. Catal. B.*, **43**, 163 (2003).
9. S. J. Castillo, M. Sotelo-Lerma, R. A. Zingaro, R. RamõÂrez-Bon, F. J. Espinoza-Beltran, R. Guillemette and M. A. DomõÂnguez, *J. Phys. Chem. Solids.*, **62**, 1069 (2001).
10. H. Jia, H. Xu, Y. Hu, Y. Tang and L. Zhang, *Electrochem. Commun.*, **9**, 354 (2007).
11. H. Xia, H. Zhuang, T. Zhang and D. Xiao, *Mater. Lett.*, **62**, 1126 (2005).
12. P. Xu, G. M. Zeng, C. L. Feng, S. Hu, M. H. Zhao, C. Lai, Z. Wei, C. Huang, G. X. Xie and Z. F. Liu, *Sci. Total Environ.*, **424**, 1 (2012).
13. J. Kiwi and M. Gratzel, *J. Chem. Soc.*, **83**, 1101 (2005).
14. S. Chatterjee, S. Sarkar and S. N. Bhattacharyya, *J. Photochem. Photobiol. A.*, **81**, 199 (1994).
15. O. Akhavan and R. Azimirad, *Appl. Catal. A.*, **369**, 77 (2009).
16. S. Kuang, L. Yang, S. Luo and Q. Cai, *Appl. Surf. Sci.*, **255**, 7385 (2009).
17. H. Liu, H. K. Shon, X. Sun, S. Vigneswaran and H. Nand, *Appl. Surf. Sci.*, **257**, 5813 (2011).
18. H. Zhao, W. Fu, H. Yang, Y. Xu, W. Zhao, Y. Zhang, H. Chen, Q. Jing, X. Qi, J. Cao, X. Zhou and Y. Li, *Appl. Surf. Sci.*, **257**, 8778 (2011).
19. Y. Jeong, M. Fan, S. Singh, C.-L. Chuang, B. Saha and J. H. v. Leeuwen, *Chem. Eng. Process.*, **46**, 1030 (2007).
20. C. Chen, J. Hu, D. Shao, J. Li and X. Wang, *J. Hazard. Mater.*, **164**, 923 (2009).
21. I. Lee, J.-A. Park, J.-K. Kang, J.-H. Kim, J.-W. Son, I.-G. Yi and S.-B. Kim, *Environ. Eng. Res.*, **19**, 157 (2014).
22. A. Idris, E. Misran and N. M. Yusof, *J. Ind. Eng. Chem.*, **18**, 2151 (2012).
23. M. Rahman, E. Misran, A. Idris and N. M. Yusof, *J. Technol.*, **67**, 5 (2014).
24. A. Idris, N. S. M. Ismail, N. Hassan, E. Misran and A.-F. Ngomsik, *J. Ind. Eng. Chem.*, **18**, 1582 (2012).
25. A. Idris and Z. Majidnia, *Desalin. Water Treat.* 1, DOI:10.1080/19443994.2014.940396 (2014).
26. R. Thapa, S. Maiti, T. H. Rana and U. N. Maiti, *J. Mol. Catal. A.*, **363**, 223 (2012).
27. A. Idris, N. Hassan, N. S. Mohd Ismail, E. Misran, N. Mohd Yusof, A. F. Ngomsik and A. Bee, *Water Res.*, **44**, 1683 (2010).
28. A. Idris, N. Hassan, R. Rashid and A. F. Ngomsik, *J. Hazard. Mater.*, **186**, 629 (2011).
29. F. Sala and F. Trifirò, *J. Catal.*, **34**, 68 (1974).
30. A. Saeed, A. M. Waheed and M. Iqbal, *Sep. Purif. Technol.*, **45**, 25 (2005).
31. A. F. Ngomsik, A. Bee, J. M. Siaugue, V. R. Cabuil and G. R. Cote, *Water Res.*, **40**, 1848 (2006).
32. R. Apiratikul, T. F. Marhaba, S. Wattanachira and P. Pavasant, *J. Sci. Technol.*, **26**, 199 (2004).
33. F. Chen, R. Shi, Y. Xue, L. Chen and Q. H. Wan, *J. Magn. Magn. Mater.*, **322**, 2439 (2010).
34. P. Mohapatra, S. K. Samantaray and K. Parida, *J. Photochem. Photobiol. A.*, **170**, 189 (2005).
35. N. Fiol, I. Villaescusa, M. Martínez, N. Miralles, J. Poch and J. Serarols, *Sep. Purif. Technol.*, **50**, 132 (2006).
36. Y. Cong, Z. Li, Y. Zhang, Q. Wang and Q. Xu, *Chem. Eng. J.*, **191**, 356 (2012).
37. S. Kuang, L. Yang, S. Luo and Q. Cai, *Appl. Surf. Sci.*, **255**, 7385 (2009).
38. Y. S. Ho and G. McKay, *Water Res.*, **33**, 585 (1999).